

CNEA Fresh Fuel Plate Characterization Summary Report

D. Keiser
F. Rice

February 2012



The INL is a U.S. Department of Energy National Laboratory
operated by Battelle Energy Alliance

CNEA Fresh Fuel Plate Characterization Summary Report

**D. Keiser
F. Rice**

February 2012

**Idaho National Laboratory
Idaho Falls, Idaho 83415**

<http://www.inl.gov>

**Prepared for the
U.S. Department of Energy
Office of Nuclear Energy
Under DOE Idaho Operations Office
Contract DE-AC07-05ID14517**

DISCLAIMER

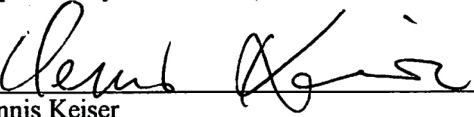
This information was prepared as an account of work sponsored by an agency of the U.S. Government. Neither the U.S. Government nor any agency thereof, nor any of their employees, makes any warranty, expressed or implied, or assumes any legal liability or responsibility for the accuracy, completeness, or usefulness, of any information, apparatus, product, or process disclosed, or represents that its use would not infringe privately owned rights. References herein to any specific commercial product, process, or service by trade name, trade mark, manufacturer, or otherwise, does not necessarily constitute or imply its endorsement, recommendation, or favoring by the U.S. Government or any agency thereof. The views and opinions of authors expressed herein do not necessarily state or reflect those of the U.S. Government or any agency thereof.

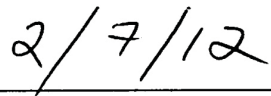
CNEA Fresh Fuel Plate Characterization Summary Report


INL/EXT-12-24722

February 2012

Approved by:

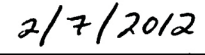

Dennis Keiser
GTRI Fuel Development Characterization Lead


Date


Mitchell Meyer
GTRI Fuel Development Technical Lead


Date


Jon Carmack
Department Manager


Date

CONTENTS

ACRONYMS	x
1. PLATE SUMMARY	1
2. INL CHARACTERIZATION OF CNEA PLATES	2
2.1 Ultrasonic Testing	2
2.2 Density and Location Radiography	3
2.3 Radiography Analysis.....	4
2.4 Thermography.....	5
2.5 Optical Microscopy (OM), Scanning Electron Microscopy (SEM), and Transmission Electron Microscopy (TEM) Analysis	7
2.6 Blister Anneal Test	12
3. SUMMARY AND CONCLUSIONS	14

FIGURES

Figure 1: The four components of a Zircaloy-clad fuel plate: Two covers, a frame, and a fuel coupon.	1
Figure 2: A fuel plate assembly.....	1
Figure 3: Radiography of CNEA plates for density.	3
Figure 4: Estimated foil thickness CNEA plates using 0.030” zirconium plate.....	4
Figure 5: Estimated foil thickness CNEA plates using 0.045” zirconium plate.....	4
Figure 6: Plate ARE10Mo1 UT image.	5
Figure 7: Plate ARE10Mo2 UT image.	5
Figure 8: Plate ARE08Mo2 UT image.	5
Figure 9: ARE10Mo1 thermography image.	6
Figure 10: ARE10Mo2 thermography image.	6
Figure 11: ARE08Mo2 thermography image.	6
Figure 12: Thermography/UT overlays for plates, ARE10Mo1, ARE10Mo2, and ARE08Mo2.	7
Figure 13: OM view of thickest end of CNEA plate ARD10Mo1.	8
Figure 14: ARD10Mo1, 50x-BSE - Low magnification SEM image of the dogbone fuel zone end with the interaction layer trailing into the cladding.	8
Figure 15: ARD10Mo1, 50x-BSE – Low magnification SEM fuel plate cross-section.	8
Figure 16: ARD10Mo1, 1kx-BSE – SEM image of the cladding/zirconium/fuel foil interface.....	8
Figure 17: ARD10Mo1, 50x-BSE – SEM image with EDS/WDS spectroscopy of the fuel foil end. The diffusion barrier and interaction layers are extending into the cladding.....	9
Figure 18: SEM image showing five locations (S1-S5) where a FIB was used to generate TEM samples.	10
Figure 19: TEM images taken from sample 2 showing the phases found at the center of the sample (a), and the phases found at the interaction layer/Zircaloy cladding interface (b).	10
Figure 20: TEM image taken from sample 3 showing Zr-rich precipitates at the UZr ₂ /Zircaloy cladding interface.	11
Figure 21: TEM image near the center of sample 3 showing the presence of many phases and some evidence of cracking (circled area).	11
Figure 22: TEM image near the center of sample 5 showing the accumulation of Mo ₂ Zr particles.	12
Figure 23: Blister images for plate ARE08Mo2.....	13
Figure 24: Blister images for plate ARE10Mo1.....	13
Figure 25: Blister images for plate ARE10Mo2.....	13
Figure 26: Blister image with highlight overlays for plates ARE08Mo2, ARE10Mo1, and ARE10Mo2.	14

TABLES

Table 1: Fuel Plate Rolling Schedule Performed at 800°C.	1
Table 2: CNEA Plate Identification Logic	2
Table 3: UT Debond Indication and Min Clad Characterization Results.....	2

ACRONYMS

BSE	Backscatter Electron
CNEA	Comisión Nacional De Energía Atómica
EDS	Electron Dispersive Spectroscopy
FIB	Focused Ion Beam
FOZ	Fuel out of Zone
INL	Idaho National Laboratory
INLO	In-Situ Lift Out
OM	Optical Microscopy
SEM	Scanning Electron Microscopy
TEM	Transmission Electron Microscopy
TIG	Tungsten Inert Gas
UCF	University of Central Florida
UT	Ultrasonic Testing
WDS	Wavelength Dispersive Spectroscopy

CNEA Fresh Fuel Characterization Summary Report

1. PLATE SUMMARY

A Zircaloy-clad fuel plate is comprised of two covers, a frame, and a U-10Mo alloy coupon (Figure 1). Both covers and the frame are 47 mm by 35 mm. The covers are 2.7 mm thick and the frame is 1.1 mm thick. The space available for an alloy coupon is 19.5 mm by 19.5 mm. The U-10Mo coupon placed in the available space is 1.2-1.3 mm in thickness. A fuel plate assembly, before rolling, is pictured in Figure 2. Each fuel plate component is cleaned and then assembled. Tungsten Inert Gas (TIG) welding is used to bond the edges of the fuel plate under He atmosphere. The rolling steps used to fabricate a fuel plate are enumerated in Table 1. Cold rolling is employed to take the fuel plate to final thickness. Finally, the fuel plate is machined, the top and bottom ends are cut using a milling machine with a diamond disc and the side borders are milled.

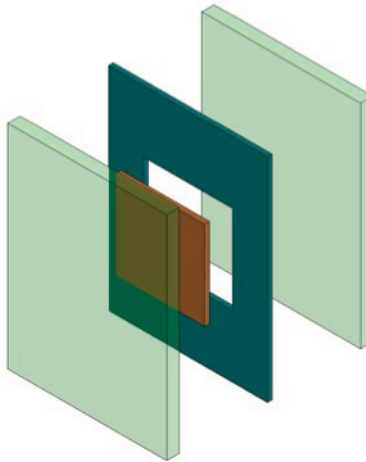


Figure 1: The four components of a Zircaloy-clad fuel plate: Two covers, a frame, and a fuel coupon.

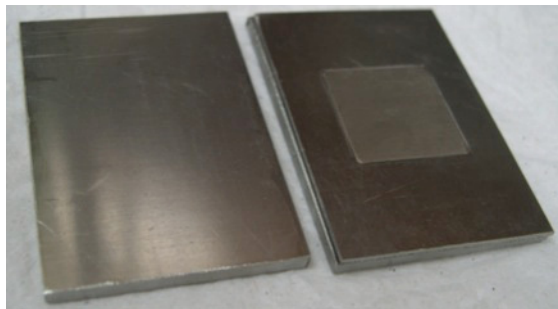


Figure 2: A fuel plate assembly.

Table 1: Fuel Plate Rolling Schedule Performed at 800°C.

Rolling Pass	Reduction %	Time (min)
0		30
1	5	15
2	5	15
3	5	15
4	9	15
5	16	15
6	23	15
7	30	15
8	28	15

2. INL CHARACTERIZATION OF CNEA PLATES




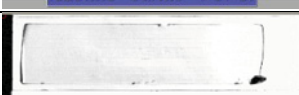


2.1 Ultrasonic Testing

Ultrasonic Testing (UT) was completed on the CNEA plates with result listed in Table 3. Plates ARE10Mo1 and ARE10Mo2 show debond indications that are greater than the tolerance of 0.06 inches (1.5 mm) stated in the specification for RERTR-13 plates. Additionally plate ARE10Mo1 has fuel out of zone (FOZ). A possible minimum cladding issue is noted on plate ARE10Mo1, where the fuel fabrication specification requires a thickness of 0.006 inches (0.15mm). All plates were included in the second phase (density and location radiography) of final processing fuel plate qualification with the assumption that Non-Compliance-Report might allow inclusion of some of the plates in the experiment. The plate naming methodology is described in Table 2.

Table 2: CNEA Plate Identification Logic

AR	E/D	08/10	1 or 2
Argentina (CNEA) Fabricated Plates	Enriched Uranium	8 wt.% Molybdenum	Plate #1
	Depleted Uranium	10 wt.% Molybdenum	Plate #2

Table 3: UT Debond Indication and Min Clad Characterization Results

Plate	UT Image	Min Clad Near side Inches (mm)	Min Clad Far side Inches (mm)	Debond Indication (Yes/No)	Pass/ Fail
ARD10Mo1		0.014 (0.35)	0.007 (0.18)	No	Pass
ARD10Mo2		0.010 (0.25)	0.012 (0.31)	No	Pass
ARE10Mo1		0.012 (0.31)	0.005 or 0.006 (0.15)	Yes	Fail
ARE10Mo2		0.007 (0.18)	0.006 (0.15)	Yes	Fail
ARE08Mo1		0.014 (0.35)	0.019 (0.48)	No	Fail (FOZ)
ARE08Mo2		0.014 (0.35)	0.017 (0.48)	Yes	Pass*

* Debond indication was small enough that the plate may have passed based on further examination, however it was ultimately rejected due to the lack of uniform fuel thickness (dogbone).

2.2 Density and Location Radiography

Density and location radiography images were obtained for the CNEA fuel plates listed in Table 3 to further characterize the viability of the plates, provide fabrication process results on final foil location, and fuel foil thickness. The plates were radiographed using the settings below:

- Light location is: 100 kv, 3.0 mA and 25 seconds
- Dark location is: 100 kv, 3.0 mA and 1.25 minutes
- Density shots are: 160 kv, 3.0 mA and 1.25 minutes
- The tube head used is a Yxlon 300 kvp and 3.0 mA Smart-tube

The plates as listed in Table 3 show the density images in Figure 3 and are labeled accordingly. All plates based on the end region thickness exceeded the maximum fuel foil thickness specification requirements.

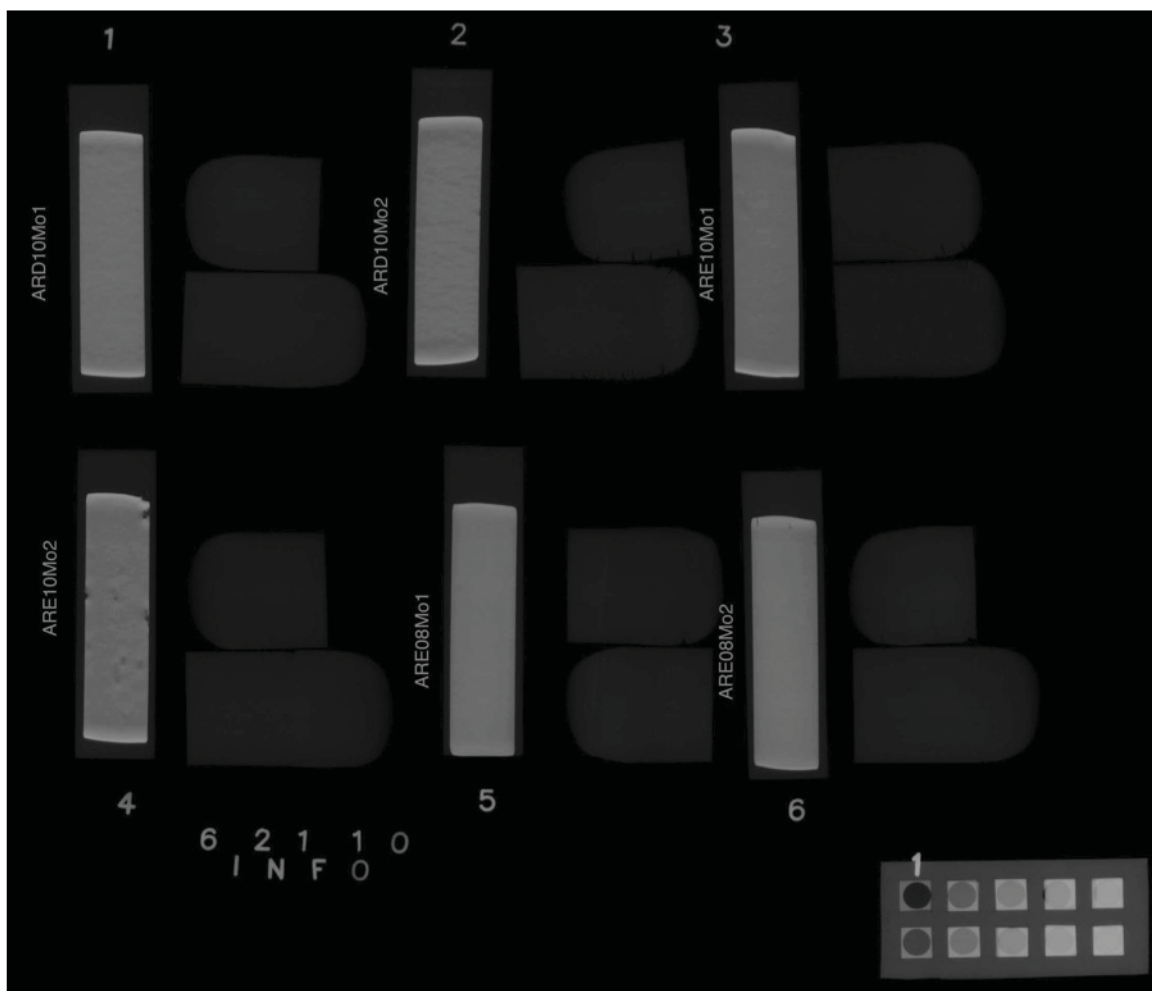


Figure 3: Radiography of CNEA plates for density.

2.3 Radiography Analysis

While the radiography density analysis method has not been applied to Zircaloy clad plates by the INL for previous experiments a method was established in this experiment that indicated non-uniform foil thicknesses. The foil thickness are indicated in the plots shown in Figure 4 and Figure 5 using a 0.030 (0.76 mm)-thick zirconium plate and a 0.045 (1.14 mm)-thick zirconium plate respectively.

While this approach was meant to address the large differences in clad thickness in the plates as indicated by the UT, there was enough error in the results that more development of this method is warranted. Optical microscopy (OM) on plate ARD10Mo1 revealed the thickest location predicted by radiography as ~20% thinner than was actually observed. The actual foil thickness on the same plate was ~30% thinner than the average from the density radiography of the non-end plate region.

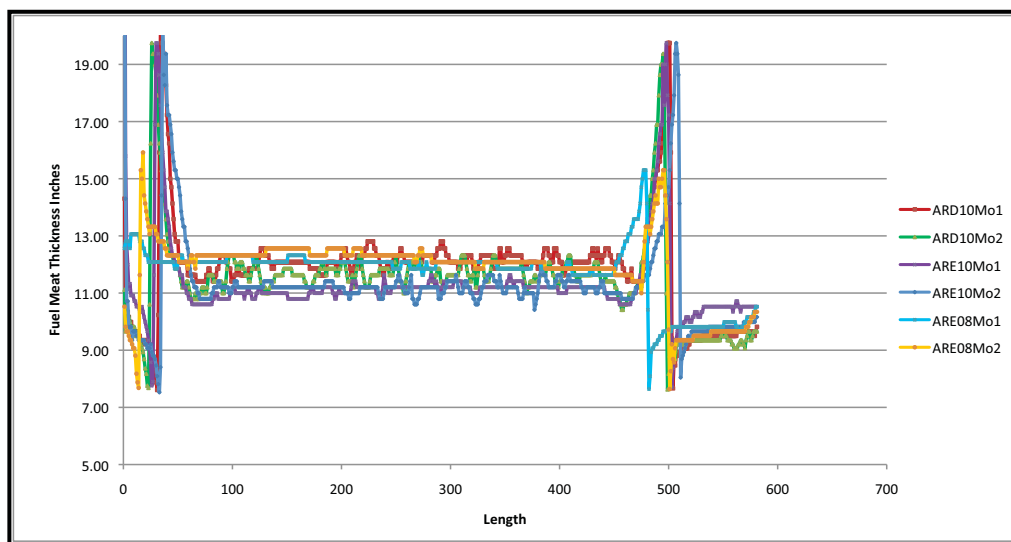


Figure 4: Estimated foil thickness CNEA plates using 0.030'' zirconium plate.

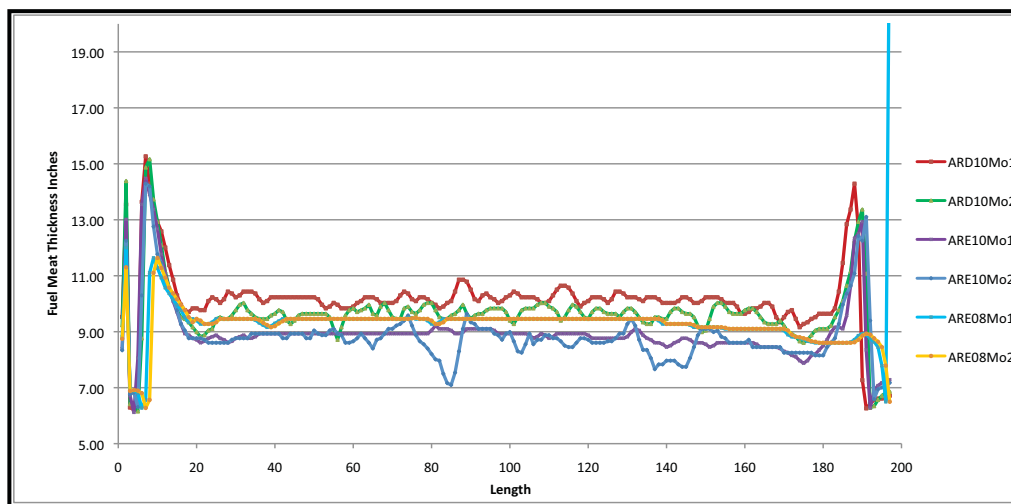


Figure 5: Estimated foil thickness CNEA plates using 0.045'' zirconium plate.

2.4 Thermography

Of the six CNEA plates, three have debond indications identified using UT. These Zircaloy clad roll bonded U-8Mo and U-10Mo plates were then examined using thermography to evaluate for debond indications. Figure 6 - Figure 8 show the debond indications as characterized using UT. Dark vertical areas at the end of the plate as shown in Figure 7 in green box and at opposite end are likely edge effects of the UT process and not necessarily considered debond indications. Areas can also be seen in Figure 6 & 7.

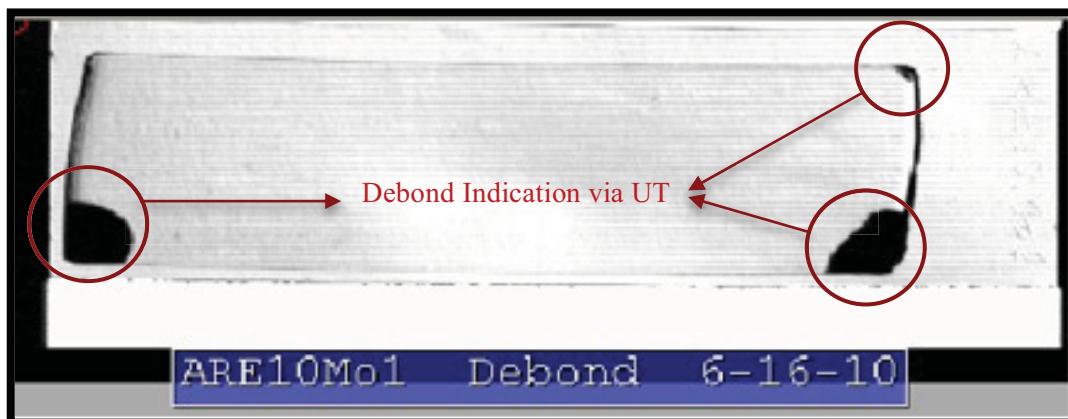


Figure 6: Plate ARE10Mo1 UT image.

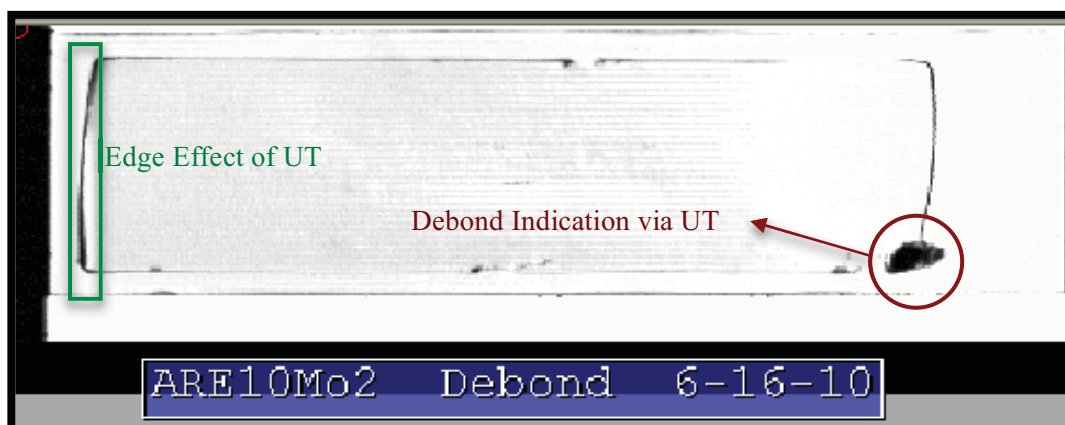


Figure 7: Plate ARE10Mo2 UT image.



Figure 8: Plate ARE08Mo2 UT image.

Thermography results for debond indication analysis are shown in Figure 9 - Figure 11. Plate ARE08Mo2 shown in Figure 11 lacks the resolution to determine if the area of interest shown is the debond indication as shown in Figure 9. Further refinement of the Thermography evaluation method may improve the resolution, however, the current approach does demonstrate the current thermography process is able to resolve larger debond indications. As indicated on plates ARE10Mo1 and ARE10Mo2 shown in Figure 9 and Figure 10, it can be seen that the resolution is sufficient to identify the larger areas of interest.

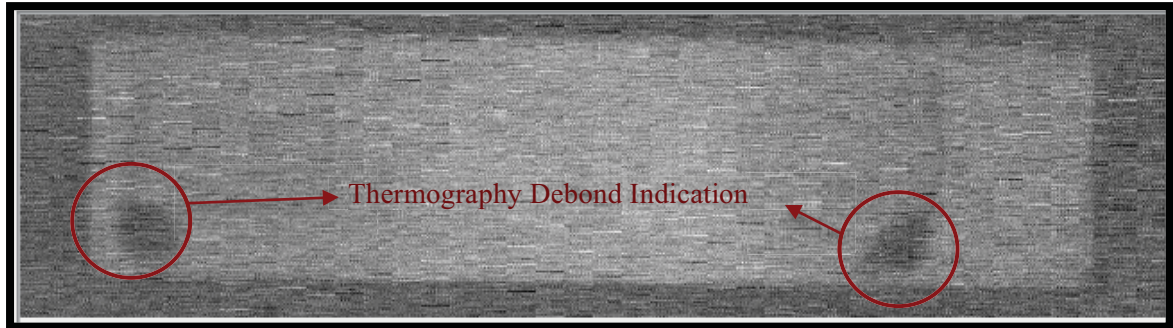


Figure 9: ARE10Mo1 thermography image.

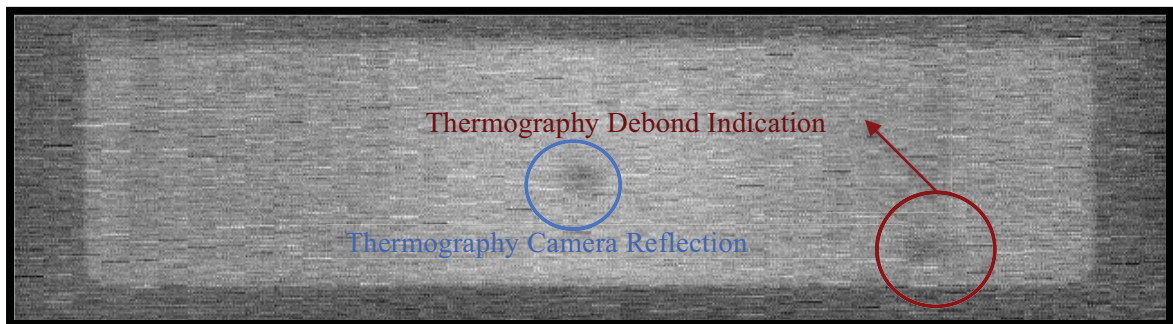


Figure 10: ARE10Mo2 thermography image.

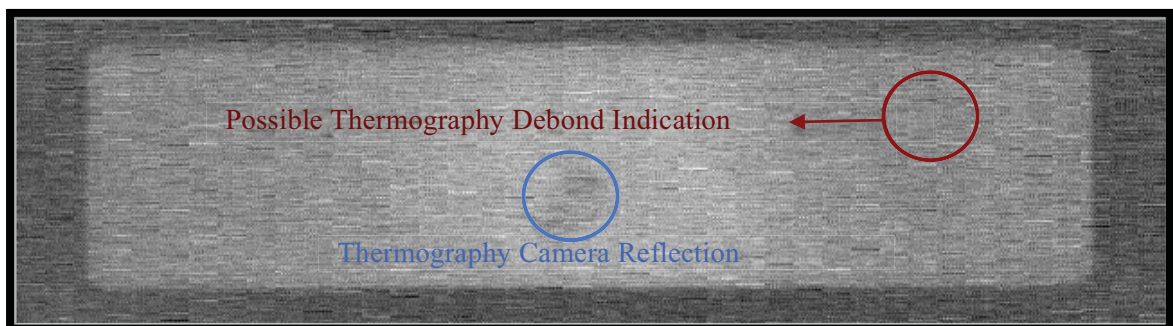


Figure 11: ARE08Mo2 thermography image.

Figure 12 shows the CNEA plates in question with the UT scans overlaid on the thermography images. This was achieved using photo editing software, where the UT debond indications (Figure 6 - Figure 8) were highlighted and overlaid onto the thermography images (Figure 9 - Figure 11) to illustrate the position of the debond indication. As indicated in Figure 11, plate ARE08Mo2 does not provide a suitable signal in the thermography analysis for detection of debond indications when the areas are smaller. This shortfall is expected to be resolved as the technology is further developed.

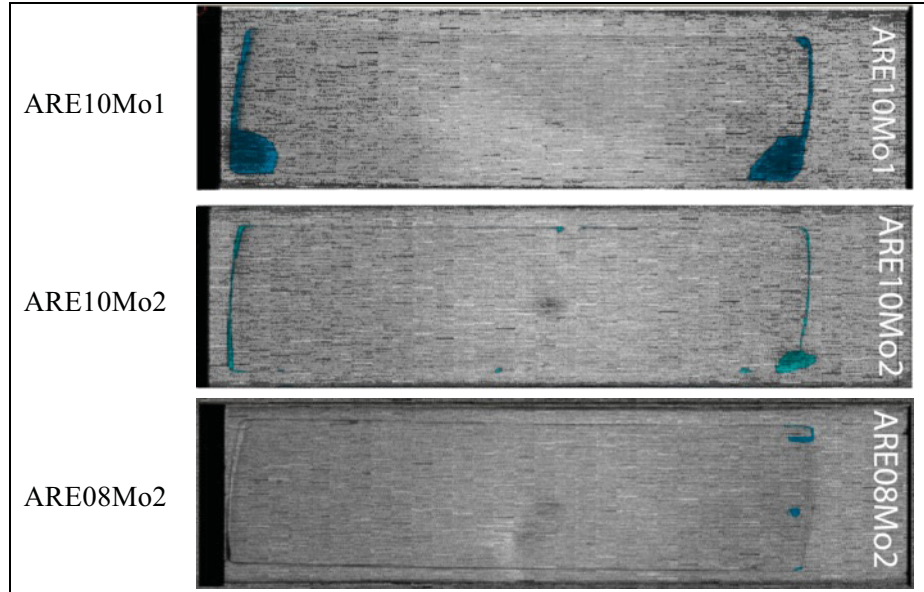


Figure 12: Thermography/UT overlays for plates, ARE10Mo1, ARE10Mo2, and ARE08Mo2.

2.5 Optical Microscopy (OM), Scanning Electron Microscopy (SEM), and Transmission Electron Microscopy (TEM) Analysis

Plate ARE10Mo1 was sectioned along the middle of the longitudinal axis to collect samples for the purpose of verifying foil thickness determined via radiography and minimum clad thickness. Figure 13 shows an optical image of the thickest dogbone fuel end of the sectioned plate. The fuel thickness at the end was determined to be $\sim 0.028''$ (~ 0.70 mm). This is $\sim 20\%$ thicker in the end region than was determined using the Zirconium plate of $0.030''$ (0.76 mm) in the density radiography shots. The minimum clad thickness in this thicker region is $\sim 0.007''$ (~ 0.18 mm) which correlates with the UT mid-clad data (see Table 3) for this plate. The main foil thickness in this section is $\sim 0.008''$ (~ 0.21 mm) where the density radiography predicted the thickness to an average in the non-end regions to be $\sim 0.012''$ (0.30 mm) across the plate.

SEM analysis with energy dispersive and wavelength dispersive spectroscopy (EDS/WDS) was performed to generate higher magnification images of the U-10Mo/Zircaloy cladding interface. Figure 14 shows a backscattered electron image of the dog-bone fuel zone. Figures 15 and 16 show images taken away from the dog-bone region. X-ray maps generated using EDS and WDS are shown in Figure 17. An interaction zone is present between the U-10 Mo alloy and the Zircaloy cladding where some areas are enriched in molybdenum and others in zirconium.



Figure 13: OM view of thickest end of CNEA plate ARD10Mo1.

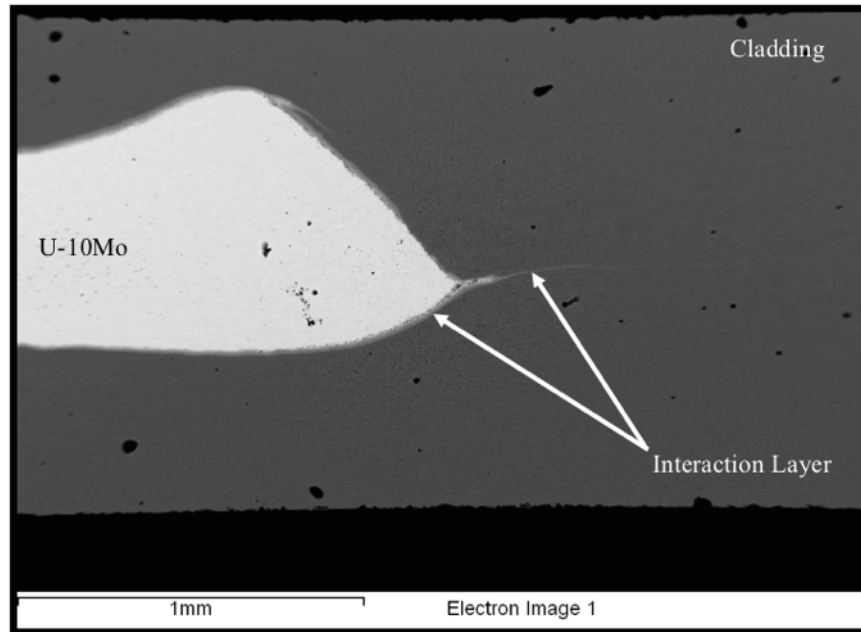


Figure 14: ARD10Mo1, 50x-BSE - Low magnification SEM image of the dogbone fuel zone end with the interaction layer trailing into the cladding.

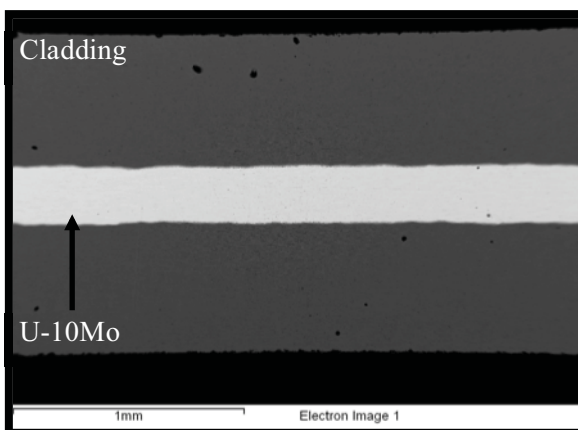


Figure 15: ARD10Mo1, 50x-BSE – Low magnification SEM fuel plate cross-section.

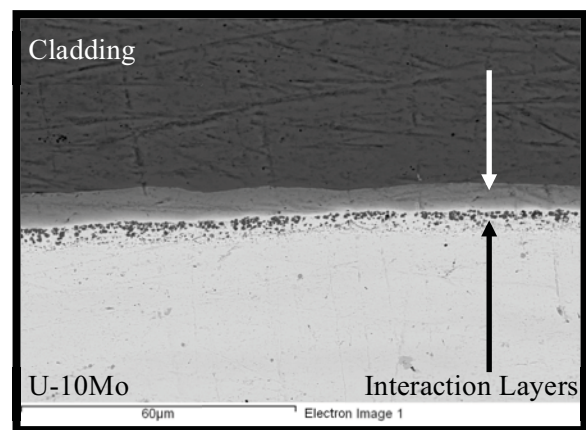


Figure 16: ARD10Mo1, 1kx-BSE – SEM image of the cladding/zirconium/fuel foil interface.

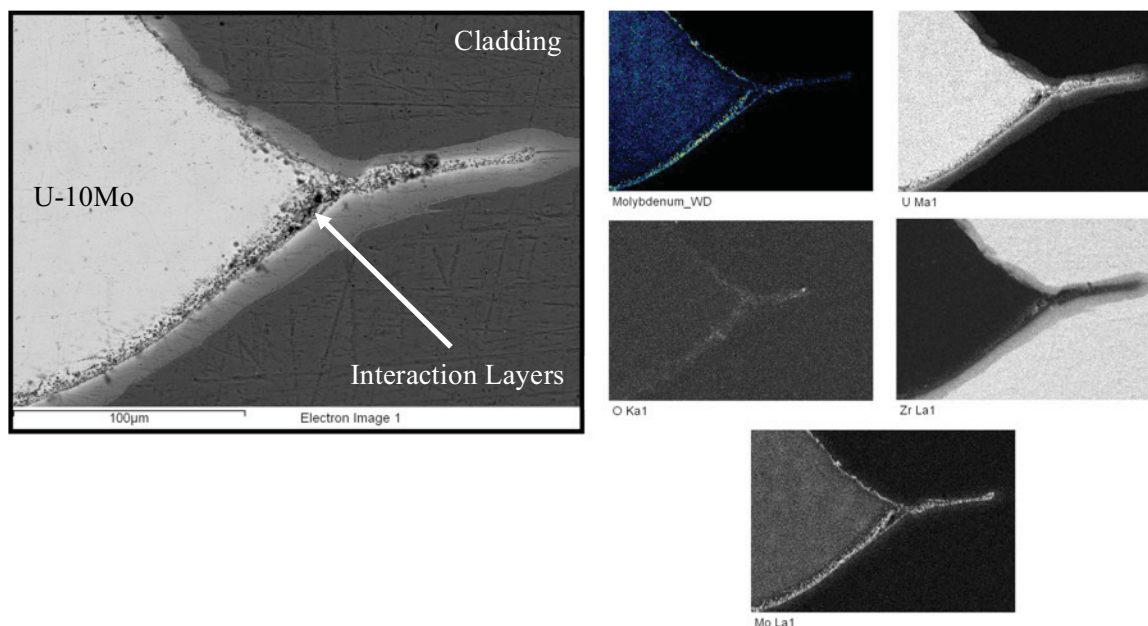


Figure 17: ARD10Mo1, 50x-BSE – SEM image with EDS/WDS spectroscopy of the fuel foil end. The diffusion barrier and interaction layers are extending into the cladding.

Samples for TEM analysis were generated using a focused ion beam/in-situ lift out (FIB/INLO) technique at the University of Central Florida (UCF). Figure 18 shows an SEM image of the five locations (S1-S5) where TEM samples were generated from the fuel plate sample. Figure 19 show TEM images taken for sample 2. The red circles indicate locations where compositions were measured, however, these values are not included in this report. At the center of the sample a multiphase area was observed consisting of a U-rich matrix phase and Mo_2Zr precipitates and layers of UZr_2 were observed on either side. At the interaction layer/Zircaloy cladding interface, zirconium-rich phase layers were observed. The crack observed at the multiphase layer/ UZr_2 layer interface was also observed in samples 3, 4, and 5. The presence of cracks in all these samples suggests that they likely formed during plate fabrication and possibly during sample polishing and not during FIB milling. The image from sample 3 (Figure 20) shows that not only zirconium-rich layers could be found at the UZr_2 /Zircaloy cladding interface but also zirconium-rich precipitates. Another image from sample 3 (Figure 21) shows the complex microstructure that can develop and the presence of cracks. The Mo_2Zr particles that were observed typically as discrete precipitates could also be found in a more layer-like form (Figure 22).

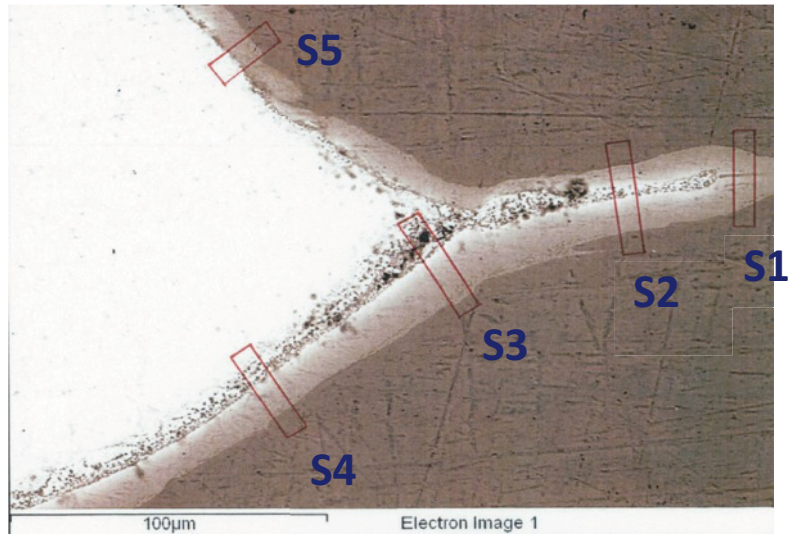


Figure 18: SEM image showing five locations (S1-S5) where a FIB was used to generate TEM samples.

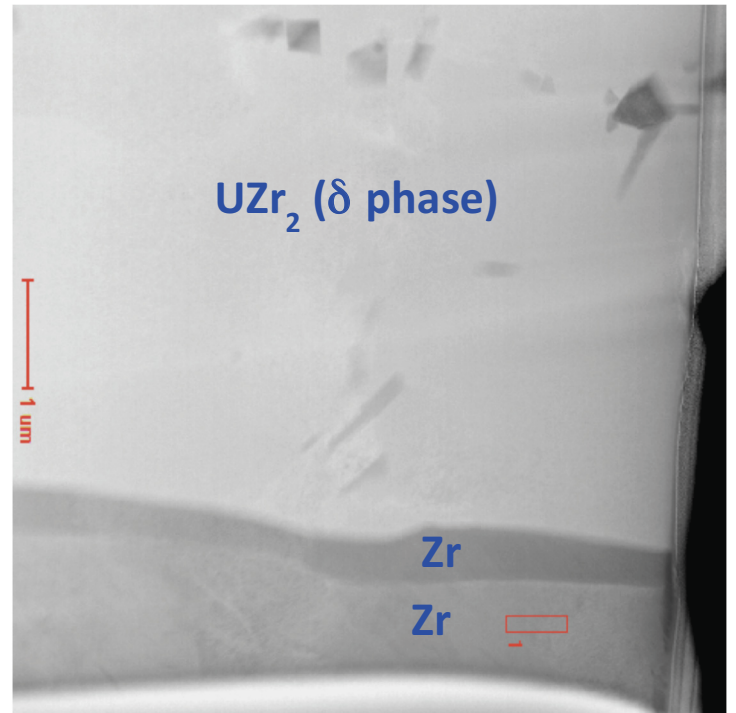
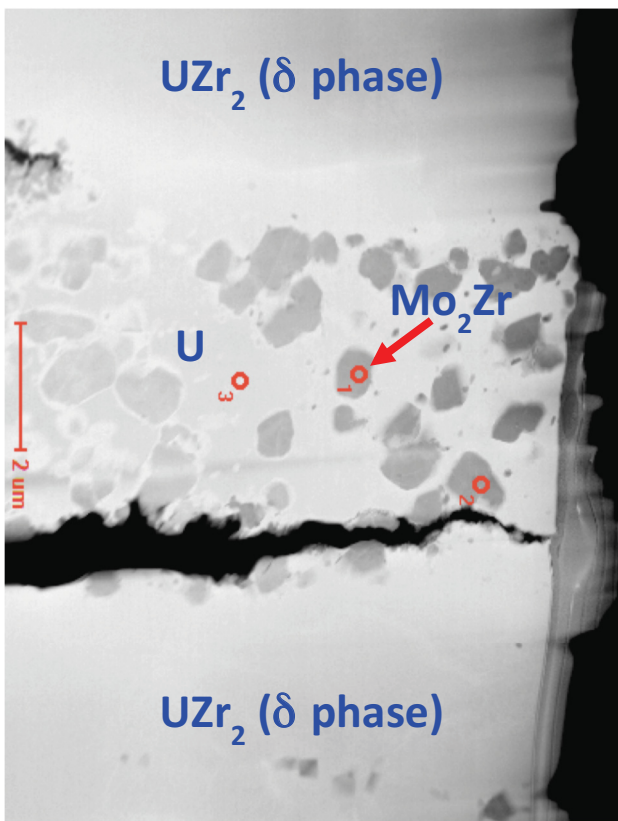


Figure 19: TEM images taken from sample 2 showing the phases found at the center of the sample (a), and the phases found at the interaction layer/Zircaloy cladding interface (b).

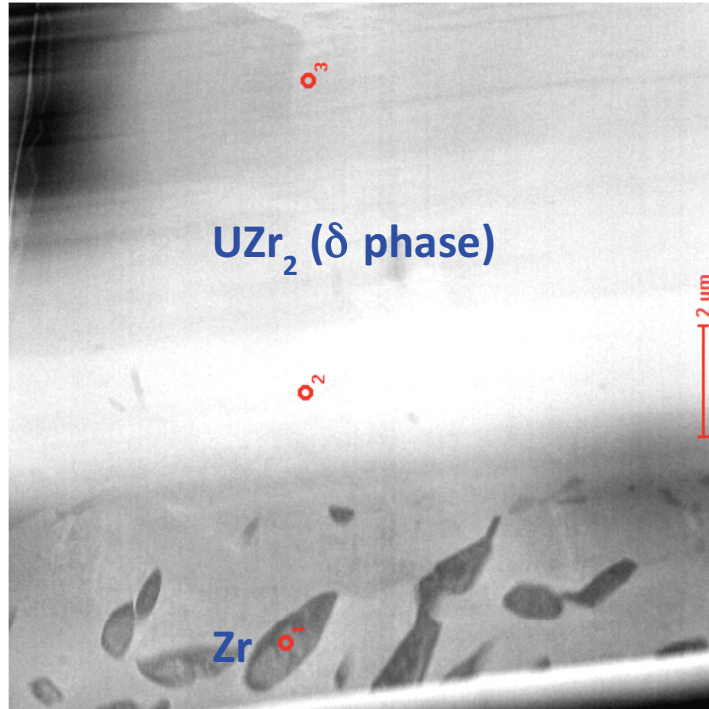


Figure 20: TEM image taken from sample 3 showing Zr-rich precipitates at the UZr_2 /Zircaloy cladding interface.

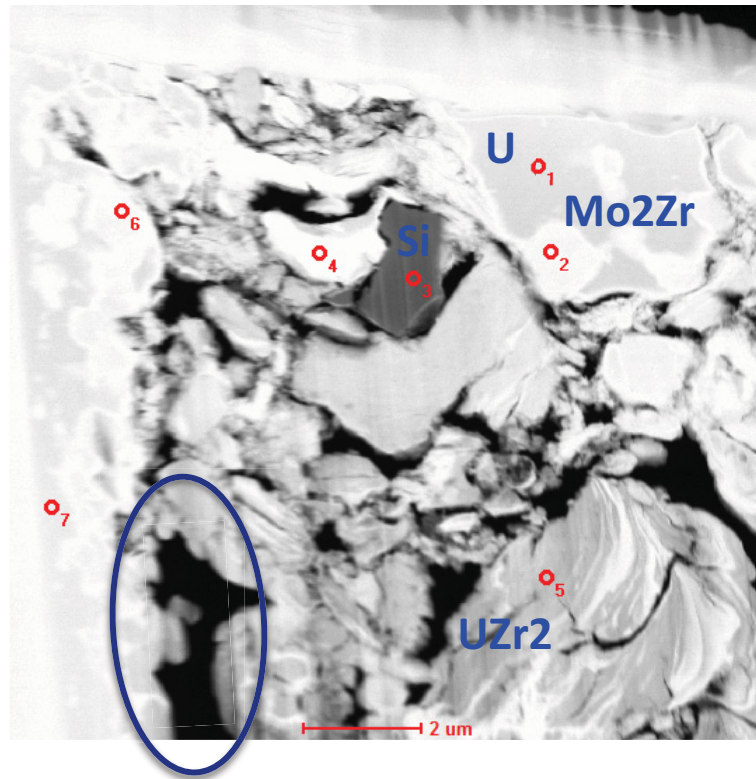


Figure 21: TEM image near the center of sample 3 showing the presence of many phases and some evidence of cracking (circled area).

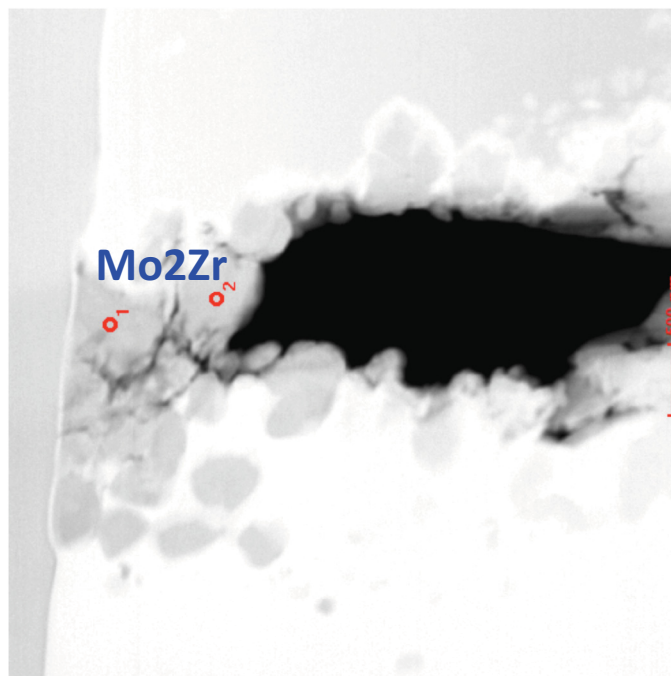


Figure 22: TEM image near the center of sample 5 showing the accumulation of Mo₂Zr particles.

2.6 Blister Anneal Test

Blister anneal testing was performed on the three plates with the debond images as indicated by UT and thermography. These plates are ARE08Mo2, ARE10Mo1 and ARE10Mo2 and the blister images are found in Figure 23 - Figure 25 (please note that backside images are flipped to line blisters up with front side images). The blister anneal test was performed in a tube furnace with plates placed in a quartz glass tube filled with air. Starting temperature was 700°C and increased in 25-degree increments until blisters formed. Hold time at each temperature was 30 minutes once temperature was reached. Ramp time between temperatures was ~5 minutes. Plates were visually inspected following the soak at each temperature but were not removed from sealed quartz tube to do so.

Plates ARE10Mo1 and ARE10Mo2 with the larger debond indication areas were showing discoloration in these areas during the inspection following the 700°C soak but the areas did not appear to be raised as would be the case if a blister had formed. Blister formation on all plates was confirmed at 825°C and the test was concluded at this point. Total test time interval was 3.5 hours.

An overlay analysis similar to that described in section 2.4 was performed on the blistered plates to define the blister areas as they relate to the UT images. These results are shown in Figure 19 for each of the plates blister annealed. Note that on plate ARE08Mo2 a blister formed in a location where there was a questionable debond indication as the darker region could have been taken as an edge effect as shown in Figure 8.



Figure 23: Blister images for plate ARE08Mo2.



Figure 24: Blister images for plate ARE10Mo1.



Figure 25: Blister images for plate ARE10Mo2.

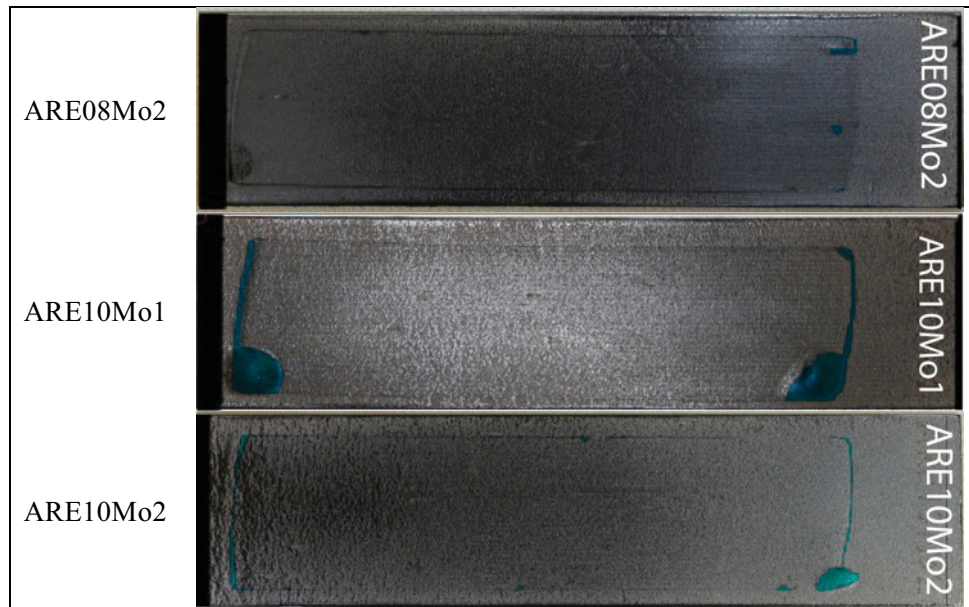


Figure 26: Blister image with highlight overlays for plates ARE08Mo2, ARE10Mo1, and ARE10Mo2.

3. SUMMARY AND CONCLUSIONS

The CNEA plates had three non-destructive evaluation (NDE) evaluations applied to the plates to assess the viability of the plates for inclusion in the RERTR-13 experiment. Ultrasonic testing revealed that several of the plates were not candidates for the experiment but it was decided to move forward with the next NDE evaluation for the purposes of providing characterization information to CNEA plate fabricators. Radiography for fuel density was performed which resulted in confirmation of the lack of uniform thickness (dogbone) at fuel ends in addition to the FOZ for plate ARE08Mo1. Thermography was performed on plates ARE08Mo2, ARE10Mo1 and ARE10Mo2 to assess the NDE method for a portable debond examination method and the technology was determined to be an acceptable method for the application.

Destructive examinations of plate ARE10Mo1 was performed to verify clad and fuel thickness data generated using UT and radiography. An OM examination of the thickest end of this plate confirmed the UT data for the min-clad value indicated and provided somewhat of a correction factor for the density data provided by radiography. Further examination of the ARE10Mo1 cross-section using SEM and EDS/WDS revealed the presence of an interaction layer at the U-10Mo/Zr interface, as well as uranium, molybdenum and oxygen enriched areas in the tailing found at the end of the dog-bone region. UCF personnel conducted TEM and FIB analysis on the plate sample. Multiphase layers were observed at the U-10Mo/Zircaloy cladding interface with evidence of cracking. Blister anneal examinations of plates ARE08Mo2, ARE10Mo1 and ARE10Mo2 produced blisters at 825°C in the debond areas that were indicated via UT and thermography in addition to a few other regions.